Appl Magn Reson (2013) 44:595–603
DOI 10.1007/s00723-012-0433-7

Applied
Magnetic Resonance

Experimental Setup for Observation the Bose–Einstein Condensation of Magnons in Solid Antiferromagnets $CsMnF_3$ and $MnCO_3$

E. M. Alakshin · Yu. M. Bunkov · R. R. Gazizulin · A. V. Klochkov · V. V. Kuzmin · R. M. Rakhmatullin · A. M. Sabitova · T. R. Safin · M. S. Tagirov

Received: 19 July 2012 / Revised: 19 October 2012 / Published online: 31 January 2013

Abstract The Bose–Einstein condensation of magnons was observed in 1984 in superfluid ^{3}He–B. The same phenomena should exist in solid magnetic systems. We describe here a partly digital experimental setup for studying solid antiferromagnets $CsMnF_3$ and $MnCO_3$ by pulse and continuous wave nuclear magnetic resonance. With this equipment, the Bose–Einstein condensation of magnons was observed for the first time in these single crystals.

1 Introduction

The Bose–Einstein condensation (BEC) corresponds to the formation of a collective quantum state in which macroscopic number of particles is governed by a single wave function. The formation of this state was predicted by Einstein in 1925 [1].

The BEC of magnons appears in a system of non-equilibrium magnons which are excited by magnetic resonance. Sometimes, the term BEC of magnons is wrongly used for a magnetic phase transition [2]. Let us stress from the beginning that there is the principal difference between the magnetic ordering in equilibrium and the BEC of quasiparticles which was discussed in Ref. [3].

In these magnetic systems, the symmetry breaking phase transition starts when the system becomes softly unstable towards the growth of one of the magnon modes. The condensation of this mode can be used for the description of the soft mechanism of the formation of ferromagnetic and antiferromagnetic states [4]. However, the final outcome of the condensation is the true equilibrium ordered

E. M. Alakshin · R. R. Gazizulin (✉) · A. V. Klochkov · V. V. Kuzmin · R. M. Rakhmatullin · A. M. Sabitova · T. R. Safin · M. S. Tagirov
Kazan Federal University, Kremlevskaya 18, 420008 Kazan, Russia
e-mail: g-rasul@yandex.ru

Yu. M. Bunkov
Institut Neel, CNRS et Universite Joseph Fourier, F-38042 Grenoble, France

state. In the same manner, the Bose condensation of phonon modes may serve as a soft mechanism of the formation of the equilibrium solid crystals [5]. But this does not mean that the final crystal state is the Bose condensate of phonons.

The BEC of non-equilibrium magnons was discovered experimentally in superfluid phase of ^{3}He–B [6]. Then six different states of superfluid ^{3}He with the BEC formation were discovered. The review of different experiments on the BEC observation is available in Refs. [7, 8]. In all cases, BEC forms on excited non-equilibrium magnons. To excite it, the pulse or continuous pumping at nuclear magnetic resonance (NMR) frequency was used.

In Ref. [9], it was as assumed that the BEC formation is also possible in solid antiferromagnets $CsMnF_3$ and $MnCO_3$. In these antiferromagnets, the hyperfine interaction of manganese atoms leads to the strong polarization of ^{55}Mn nuclei, so its precession frequency is on the order of 600 MHz. This frequency is comparable with the low frequency mode of antiferromagnetic resonance (AFMR) in low external magnetic field. As a result, there is the coupled nuclear-electron precession with the dynamical frequency shift (pulling). From experiments carried out with ^{3}He, it is clear that the magnon BEC formation is a consequence of the analogous frequency shift, which supply the repulsive interaction between magnons, which is mandatory condition for a BEC formation. In the case of the attractive interaction, usual for magnetically ordered systems, the different types of instability destroy the coherent states. That is why the attempt to observe the magnons BEC formation in antiferromagnets $CsMnF_3$ and $MnCO_3$ was a prospective task. Our experimental setup for this research is described here.

2 Resonator

For studying NMR at frequencies of 500–600 MHz, the traditionally used radio-frequency (RF) solenoidal coils cannot provide the necessary Q-factor and the sufficient filling factor. That is why it was offered to use the split-ring (loop-gap) resonator [10, 11].

The samples were placed in the split-ring resonator (Figs. 1, 2) at the maximum magnetic field site. The experimentally determined Q-factor of the resonator was $Q \approx 150$ at the temperature of 1.5 K. Excitation of the resonator and signal detection were performed using ring antennas, matched with the cavity for 50 Ohm. The matching was achieved by adjusting the optimal antenna radius and the optimal distance between antennas and the resonator.

The samples volume was a few cubic millimeters, the resonator volume was $V \approx 308$ mm^3. The antennas diameter was about 5 mm, the distance between antenna and resonator was about 4.5 mm.

The magnetic component of the RF field, created by ring antenna, was polarized along the resonator axis. The amplitude of the magnetic component is well described by

$$H_1^2 \approx \frac{8\pi QP}{fV}, \tag{1}$$

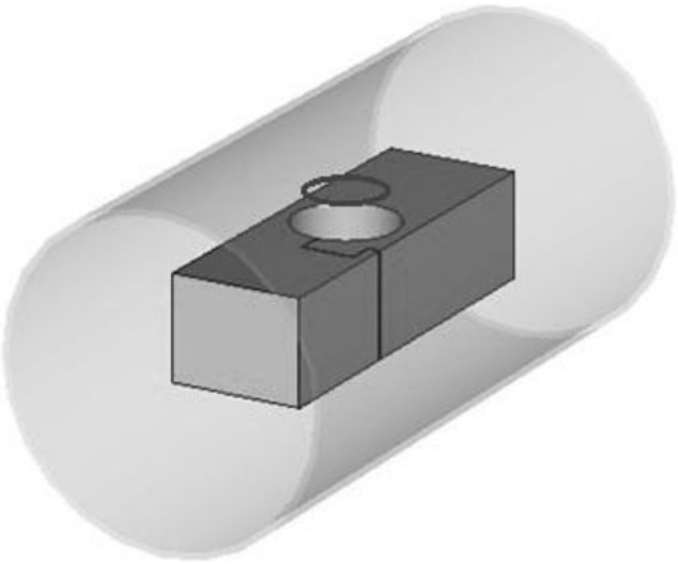

Fig. 1 Geometry of the ring antenna and the split-ring resonator

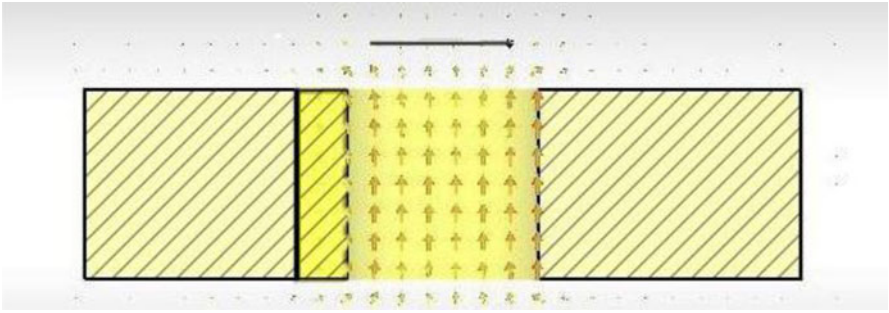

Fig. 2 Distribution of the magnetic field B_1 in the resonator calculated with the help of CST Microwave Studio program

where P,supplied RF power; f is the resonator frequency. In our experiments, the supplied RF as a result, at the resonant frequency of 566 MHz, the RF field amplitude was about 3 Oe.

The accurate calculations of the electromagnetic fields were done using CST Microwave Studio program. The Transient Solver in standard settings was used for finding the resonance, the parameters of the scattering matrix S_{11}, and the structures of the electromagnetic fields. The condition of the critical coupling was determined by changing the values of S_{11} and $\mathrm{Arg}(S_{11})$ as a function of the distance between antenna and resonator. The losses in resonator walls and dielectric material in the gap were taken into account in calculations. The electric properties of the materials were taken from the library in CST Microwave Studio. The material of the resonator

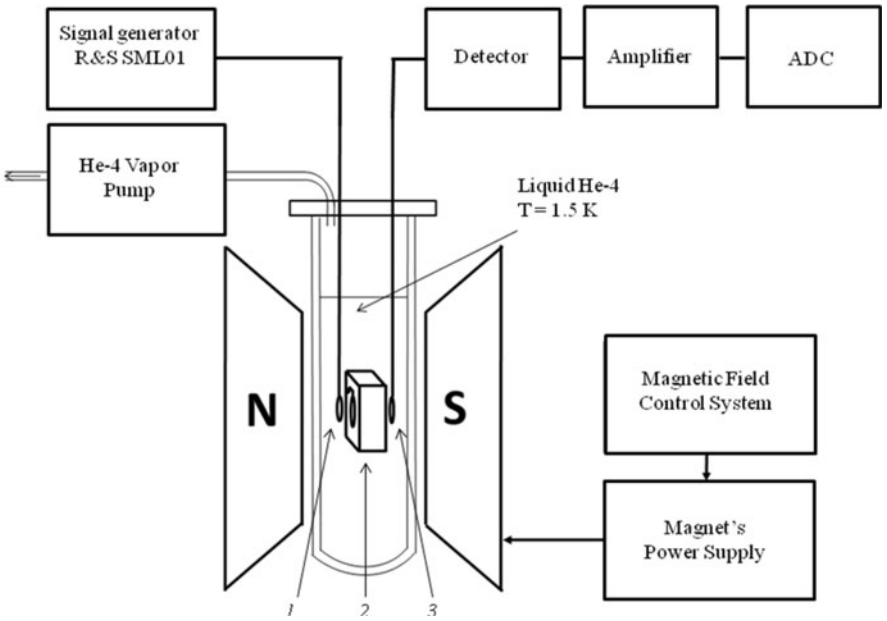

Fig. 3 Scheme of the high-frequency CW NMR spectrometer (*1*, *3*—ring antennas, *2*—resonator)

is copper, the dielectric material in the gap is the Pyrex glass with the specially selected value of the loss tangent. It was assumed that the electrostatic shield was the ideal conductor without losses because account of losses typical for copper did not significantly change the results.

The frequency range in the calculations was from 300 to 1,500 MHz. The calculated value of the resonant frequency was 559.2 MHz which is in good agreement with measured value of 560 MHz. The calculated quality factor 173 is also in good agreement with measured value of 150. At the input generator power 100 mW, the magnetic field amplitude in the rotating frame was 0.5 Oe which agrees well with calculations using Eq. (1).

3 Continuous-Wave Radiation

A scheme of the experimental setup for continuous-wave (CW) studies is shown in Fig. 3. The resonator and antennas were placed in a cryostat filled with liquid helium. The sample temperature was 1.5 K.

For CW experiments, the signal generator Rohde&Schwarz SML01 was used. The magnetic field sweeping was done by the control system which sets the value of the current through the coil of the electromagnet. The radiation power was 40 mW. The signal generator Rohde&Schwarz SML01 was controlled by PC via RS232 interface.

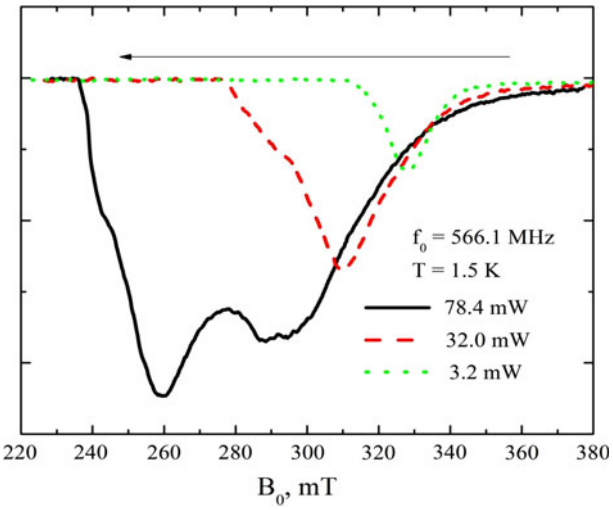

Fig. 4 Amplitude of ^{55}Mn NMR absorption signal in $CsMnF_3$ as a function of the external magnetic field for different radiation energies

The response of the spin system was detected by the loop antenna and the detector. After amplifying by the Direct Current Amplifier (DCA), the signal was digitized by the Analog-to-Digital Converter (ADC) BORDO B-211, "AURIS" Inc., with time resolution of 500 μs. The magnetic field sweeping time was about 30 s. The range of the magnetic field sweep was about 200 mT (from 300 to 500 mT). The detected signal consisted of the absorption signal and the dispersion signal. By adjustment of the cable length, we were able to detect the absorption signal predominantly (Fig. 4). At small excitation amplitudes, we detected the linear NMR signal which is formed only in the resonance field at the RF pumping frequency. The line width is defined by inhomogeneous broadening when spins precess with the local frequencies determined by the local magnetic field and interactions. The situation completely changes when we increase the pumping power. The precession frequency is locked by the RF field. The signal is observed even when the magnetic field is far away from resonance. We observe the signal amplitude increase which corresponds to the BEC formation.

The experimental setup described above was used for the magnon BEC formation and its investigation in antiferromagnets $CsMnF_3$ and $MnCO_3$. The results of these experiments and the detailed explanation of the magnon BEC formation were published in Refs. [12, 13]. It is important to point out that it is not necessary to use the double modulation techniques for the investigation of such substrates because the existence of the ordered electron spin system leads to the enormous enhancement (10^2–10^3) of the nuclei signal due to hyperfine interaction. Our setup has the possibility of fast (about 1 s) turn off and then turn on the RF radiation during the magnetic field sweeping. This was significant for studying the dynamics of the BEC formation. In addition, we were able to stop the field sweep at any time

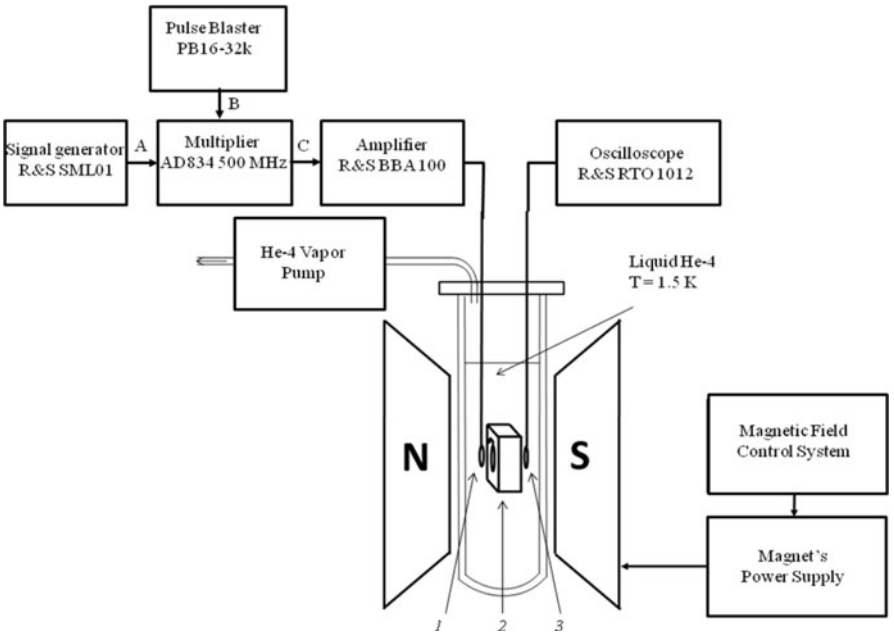

Fig. 5 Scheme of the pulse NMR spectrometer (*1*, *3*—ring antennas, *2*—resonator)

during measurements. It allowed us to understand that the BEC state is stable against overheating of the nuclear spin system [12, 13].

4 Pulse Radiation

To get a strong confirmation of the existence of the magnon BEC in our substrates, it was also necessary to study the free induction decay (FID) signal, as it has been done in earlier experiments with liquid ^{3}He–A [14]. For this purpose, we have modified our setup (Fig. 5).

The experiments were carried out at the temperature of 1.5 K. The external magnetic field was about 450 mT. The RF signal from the Rohde&Schwarz SML01 generator was applied to the input A of the multiplier AD834. Programmed by PC, the Pulse Blaster PB16-32k, SpinCore Technologies Inc., was connected to the input B. As a result, at the output C of the multiplier, we obtained the RF pulses with the filling frequency equal to the Rohde&Schwarz SML01 generator frequency. After the Rohde&Schwarz BBA100-C125 amplifier, the video pulses were applied to the loop antenna and excited the spin system. The response of the spin system was observed on the digital oscilloscope Rohde&Schwarz RTO1012 at the NMR frequency of the order of 560 MHz.

Using the Pulse Blaster PB16-32k with the amplifier Rohde&Schwarz BBA100-C125 (the maximum pulse power up to 125 W) in our equipment made it possible to vary the pulse length in a very wide range, from 0.5 μs to 10 s. The pulse edge time

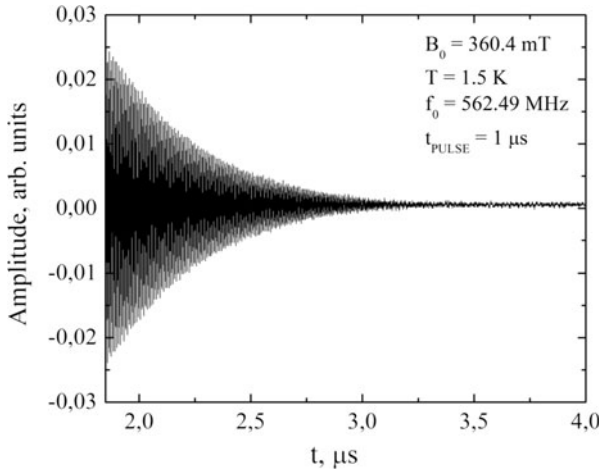

Fig. 6 Example of the free induction decay signal of ^{55}Mn in $CsMnF_3$ at linear resonance conditions

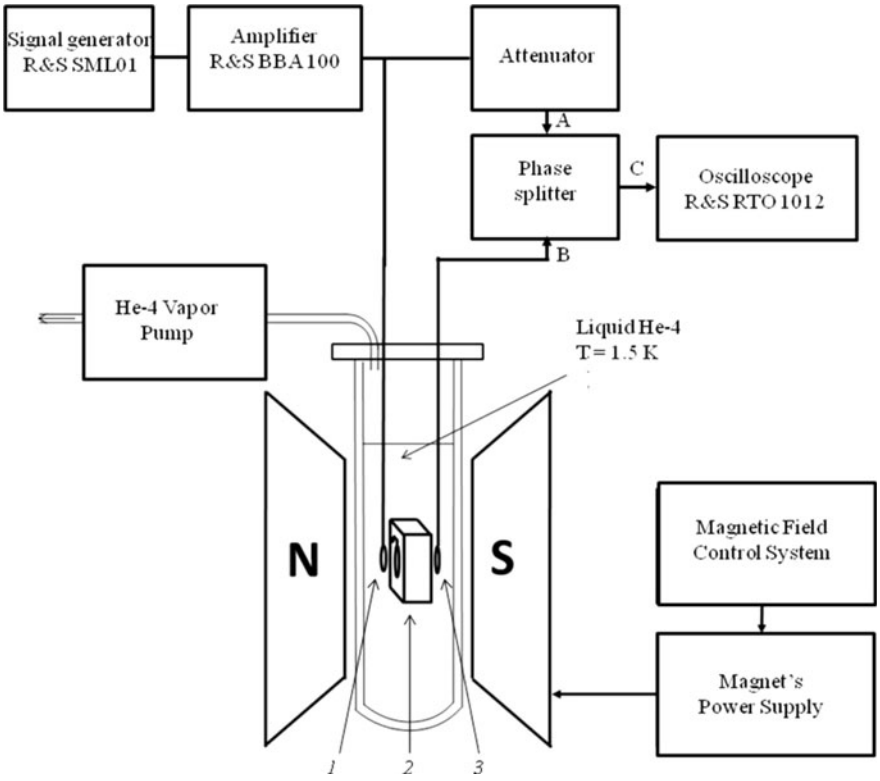

Fig. 7 Scheme of the spectrometer for the BEC formation study (*1*, *3*—ring antennas, *2*—resonator)

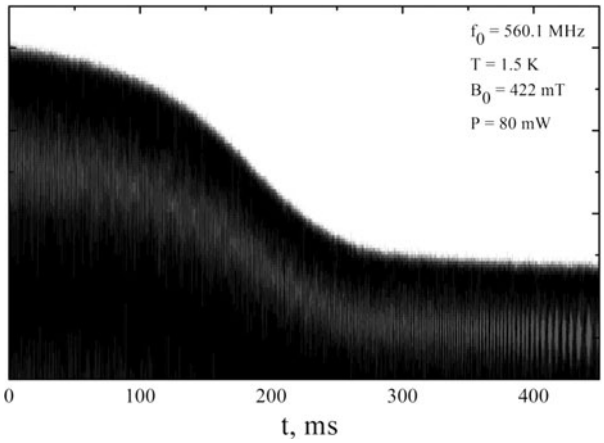

Fig. 8 Process of the BEC formation after switching on the RF radiation at time $t = 0$ in $CsMnF_3$

was about 0.1 μs. These factors played a crucial role in obtaining a strong confirmation of the magnon BEC formation in investigated substrates [15] because for creating the magnon BEC and detecting its radiation, it was necessary to apply the long and intense RF field. The example of the signal obtained by the pulse method in the linear regime is given in Fig. 6.

With the help of the compensation scheme illustrated in Fig. 7, we were able to observe directly the absorption signal formation just after turning on the RF radiation (Fig. 8).

In our scheme, the RF radiation was applied at the same time to the loop antenna and to the input A of the phase splitter after attenuation. The signal from the loop antenna goes to the input B of the phase splitter. As a result, there is a compensation of the CW RF radiation up to 70 % at the output C. This made it possible to investigate with good accuracy the response of the spin system at the high-frequency digital oscilloscope Rohde&Schwarz RTO 1012. For correct work, it was necessary that the signals at the inputs A and B were in phase. In our realization it was achieved by the accurate selection of the cable lengths.

In Fig. 8, one can see the transition process during which the magnons are slowly excited and condensed to the final coherent BEC state during about 250 ms. Observing time of the signal formation is bigger than any relaxation processes in the sample (Fig. 6) but is comparable with the pulse lengths after which the coherent magnon BEC radiation was observed [15].

5 Conclusion

We have developed and described here the experimental setup which allowed us for the first time to observe the magnon Bose–Einstein condensation in solid antiferromagnets $CsMnF_3$ and $MnCO_3$. Using the modern digital technique helped us to study the BEC dynamics by fast turn off the RF pumping during the field

sweeping, we were able to detect very slow processes such as the BEC formation. The pulse length could be varied in a wide range from 1 μs to 10 s, so we could study the BEC radiation after the long pulses (longer than 1 s).

Acknowledgments We are grateful to Rene Tschaggellar (ETH, Zurich) for calculations of the electromagnetic fields in resonator. This work is partly supported by the Ministry of Education and Science of the Russian Federation (project no. 13.G25.31.0025).

References

1. S. Giorgini, L.P. Pitaevskii, S. Stringari, Rev. Mod. Phys. **80**, 1215 (2008)
2. T. Giamarchi, Ch. Ruegg, O. Tchernyshyov, Nat. Phys. **4**, 198 (2008)
3. Yu.M. Bunkov, G.E. Volovik, Spin superfluidity and magnon Bose-Einstein condensation, ed. by K. Bennemann, J. Ketterson. Novel Superfluids (Oxford Univ. press, 2012), arxiv: 1003.4889v3 (2012)
4. T. Nikuni, M. Oshikawa, A. Oosawa, H. Tanaka, Phys. Rev. Lett. **84**, 5868 (2000)
5. W. Kohn, D. Sherrington, Rev. Mod. Phys. **42**, 1 (1970)
6. A.S. Borovik-Romanov, Yu.M. Bunkov, V.V. Dmitriev, Yu.M. Mukharskii, JETP Lett. **40**, 1033 (1984)
7. Yu.M. Bunkov, G. Volovik, J. Phys, Condens. Matter **22**, 164210 (2010)
8. Yu.M. Bunkov, in Progress of Low Temperature Physics, 14, 68, ed. by W.P. Halperin, (Elsevier Science, Amsterdam 1995)
9. Yu.M. Bunkov, Phys. Usp. **180**, 884 (2010)
10. B.S. Dumesh, Prib. Tekh. Eksp. **1**, 135 (1986)
11. W.N. Hardy, L.A. Whitehead, Rev. Sci. Instrum. **52**, 213 (1981)
12. Yu.M. Bunkov, E.M. Alakshin, R.R. Gazizulin, A.V. Klochkov, V.V. Kuzmin, T.R. Safin, M.S. Tagirov, JETP Lett. **94**, 68 (2011)
13. Yu.M. Bunkov, E.M. Alakshin, R.R. Gazizulin, A.V. Klochkov, V.V. Kuzmin, A.S. Nizamutdinov, T.R. Safin, M.S. Tagirov, J. Phys: Conf. Series **324**, 012006 (2011)
14. P. Hunger, Yu.M. Bunkov, E. Collin, H. Godfrin, J. of Low Temp. Phys. **158**, 129 (2010)
15. Yu.M. Bunkov, E.M. Alakshin, R.R. Gazizulin, A.V. Klochkov, V.V. Kuzmin, V.S. L'vov, M.S. Tagirov, Phys. Rev. Lett. **108**, 177002 (2012)